Metadata of the chapter that will be visualized in SpringerLink

Book Title	Proceedings of 2021 International Conference on Medical Imaging and Computer-Aided Diagnosis (MICAD 2021)	
Series Title		
Chapter Title	Quantification of Epicardial Adipose Tissue in Low-Dose Computed Tomography Images	
Copyright Year	2022	
Copyright HolderName	The Author(s), under exclusive license to Springer Nature Singapore Pte Ltd.	
Corresponding Author	Family Name	**Goncharov**
	Particle	
	Given Name	**Mikhail**
	Prefix	
	Suffix	
	Role	
	Division	
	Organization	Skolkovo Institute of Science and Technology
	Address	Moscow, Russia
	Email	m.belyaev@skoltech.ru
Author	Family Name	**Chernina**
	Particle	
	Given Name	**Valeria**
	Prefix	
	Suffix	
	Role	
	Division	
	Organization	Research and Practical Clinical Center for Diagnostics and Telemedicine Technologies of the Moscow Health Care Department
	Address	Moscow, Russia
	Email	
Author	Family Name	**Pisov**
	Particle	
	Given Name	**Maxim**
	Prefix	
	Suffix	
	Role	
	Division	
	Organization	Skolkovo Institute of Science and Technology
	Address	Moscow, Russia
	Email	
Author	Family Name	**Gombolevskiy**
	Particle	
	Given Name	**Victor**
	Prefix	

	Suffix	
	Role	
	Division	
	Organization	Research and Practical Clinical Center for Diagnostics and Telemedicine Technologies of the Moscow Health Care Department
	Address	Moscow, Russia
	Email	
Author	Family Name	**Morozov**
	Particle	
	Given Name	**Sergey**
	Prefix	
	Suffix	
	Role	
	Division	
	Organization	Research and Practical Clinical Center for Diagnostics and Telemedicine Technologies of the Moscow Health Care Department
	Address	Moscow, Russia
	Email	
Author	Family Name	**Belyaev**
	Particle	
	Given Name	**Mikhail**
	Prefix	
	Suffix	
	Role	
	Division	
	Organization	Skolkovo Institute of Science and Technology
	Address	Moscow, Russia
	Email	

Abstract	The total volume of Epicardial Adipose Tissue (EAT) is a well-known independent early marker of coronary heart disease. Though several deep learning methods were proposed for CT-based EAT volume estimation with promising results recently, automatic EAT quantification on screening Low-Dose CT (LDCT) has not been studied. We first systematically investigate a deep-learning-based approach for EAT quantification on challenging noisy LDCT images using a large dataset consisting of 493 LDCT and 154 CT studies from 569 subjects. Our results demonstrate that (1) 3D U-net precisely segment the pericardium interior region (Dice score 0.95 ± 0.00); (2) postprocessing based on narrow 1-mm Gaussian filter does not require adjustments of EAT Hounsfield interval and leads to accurate estimation of EAT volume (Pearson's R 0.96 ± 0.01) comparing to CT-based manual EAT assessment for the same subjects.

Keywords (separated by '-')	Epicardial fat - Low-dose CT - Deep learning

Quantification of Epicardial Adipose Tissue in Low-Dose Computed Tomography Images

Mikhail Goncharov[1(✉)], Valeria Chernina[2], Maxim Pisov[1], Victor Gombolevskiy[2], Sergey Morozov[2], and Mikhail Belyaev[1]

[1] Skolkovo Institute of Science and Technology, Moscow, Russia
m.belyaev@skoltech.ru
[2] Research and Practical Clinical Center for Diagnostics and Telemedicine Technologies of the Moscow Health Care Department, Moscow, Russia

Abstract. The total volume of Epicardial Adipose Tissue (EAT) is a well-known independent early marker of coronary heart disease. Though several deep learning methods were proposed for CT-based EAT volume estimation with promising results recently, automatic EAT quantification on screening Low-Dose CT (LDCT) has not been studied. We first systematically investigate a deep-learning-based approach for EAT quantification on challenging noisy LDCT images using a large dataset consisting of 493 LDCT and 154 CT studies from 569 subjects. Our results demonstrate that (1) 3D U-net precisely segment the pericardium interior region (Dice score 0.95 ± 0.00); (2) postprocessing based on narrow 1-mm Gaussian filter does not require adjustments of EAT Hounsfield interval and leads to accurate estimation of EAT volume (Pearson's R 0.96 ± 0.01) comparing to CT-based manual EAT assessment for the same subjects.

AQ1

Keywords: Epicardial fat · Low-dose CT · Deep learning

1 Introduction

Coronary heart disease (CHD) remains the leading cause of death and disability worldwide [8]. The primary pathological process leading to the development of CHD is coronary artery atherosclerosis, an inflammatory disease associated with lipid deposits in the vascular walls [1]. According to the results of the Multi-Ethnic Study of Atherosclerosis (MESA), the amount of adipose tissue surrounding the heart - pericardial adipose tissue - is an independent predictor of CHD [4]. Pericardial adipose tissue includes epicardial adipose tissue (EAT) located inside the pericardial contour and paracardial adipose tissue located outside and adjacent to the pericardium.

For a long time, CHD is asymptomatic and manifests at late stages with myocardial infarction or sudden death, so it is crucial to determine disease predictors even before the symptoms appear. The primary approach to addressing

R. Su et al. (Eds.): MICAD 2021, LNEE 784, pp. 1–10, 2022.
https://doi.org/10.1007/978-981-16-3880-0_11

this issue is the organization of mass preventive examinations. Since "large-scale screening" excludes the use of invasive diagnostic methods due to labor intensity, high cost, and risks of complications, the possibilities of noninvasive diagnostic techniques have attracted wide attention from the scientific community. EAT can be assessed by echocardiography (EchoCG), computed tomography (CT), and magnetic resonance imaging (MRI). EchoCG is not an optimal method to quantify EAT because of low reproducibility [9]. Cardiac MRI is an expensive and time-consuming procedure [5]. Traditionally, EAT is assessed by CT scan triggered by an electrocardiogram (ECG) with or without intravenous contrast agent [15]; non-ECG CT scan can also be used for EAT quantification as a reliable and reproducible predictor for CHD [17].

Recently, several deep-learning-based methods were proposed for EAT quantification for non-ECG-triggered CT scans. The majority of works consist of two steps: (1) pericardium delineation or segmentation of Pericardium Interior Region (PIR) segmentation followed by (2) estimation of EAT mask by simple thresholding of Hounsfield Units (HU). Also, a simple median filter is used for CT to suppress noise before thresholding in many works. A comprehensive approach with two convolutional neural networks was proposed in [2] and later replaced by a single multitask network in [3], subsequent work of the same authors. In both works, EAT quantification perfectly correlated with manual estimation (Pearson's R was 0.97). At the same time, a simpler 3D U-Net with attention was successfully used in [7] where authors reported Dice score 0.85 ± 0.05 for a small training sample of 40 subjects.

However, standard CT is associated with high radiation exposure and can not be used for screening. At the same time, as EAT reflects early signs of the disease, an automatic tool for a screening examination such as low-dose chest CT (LDCT) is required. To date, there have been only a few studies demonstrating the possibility of using non-ECG-gated low-dose chest CT for EAT volumetry [11,19]. However, these studies use labor- and time-consuming semi-automatic techniques, which complicates their implementation within clinical settings. The previously described automatic technique had been validated only for standard ECG-gated CT, not used for screening [2]. Finally, despite substantial progress in researching CT-oriented methods, automatic LDCT-based EAT volumetry in screening patients remains highly relevant.

From the technical point of view, LDCT is much noisier than CT, and this difference may affect both abovementioned steps of the pipeline

1. Worse quality of images may result in deterioration of pericardium detection or PIR segmentation quality.
2. Presence of noise may make EAT mask estimation via thresholding more challenging. Besides, the difference in scanning protocol may result in a systematic shift of HU intensities, as was shown for EAT quantification in [12] where a modified upper HU threshold showed the best match with CT-based estimations.

We aim to study both effects systematically to validate the deep learning-based method's applicability for automatic estimation of EAT volume on LDCT.

Our contributions are as follows. **(1)** We first developed and tested a pipeline for EAT quantification in LDCT. **(2)** We show that a simple 3D Unet achieves the excellent quality of PIR segmentation approaching expert's variability. **(3)** We studied several post-processing approaches and identified that (a) popular median filtering results in a systematic shift of intensities and (b) a Gaussian filter with the standard EAT HU-range provides an excellent EAT estimation with Pearson's R 0.96 ± 0.01 comparing to CT-based manual EAT assessment for the same subjects.

2 Data

Our data includes standard-dose chest CT and LDCT; the latter images were collected within a lung cancer screening pilot [16]; the radiation dose for all cases is less than one mSv. Scanning with both CT types was performed on Toshiba Aquilion 64 (Canon medical systems, Japan), with a rotation time of 0.5 sec, slice thickness 1 mm, and convolution kernel (FC07, FC51). The main differences between CT and LDCT protocols were (1) voltage: 120 kV vs. 135 kV, (2) X-ray tube current: automatic tube modulation vs. up to 25 mA, and (3) radiation dose: 7–8 mSv vs. less than 1 mSv.

Some CT and LDCT images (see details below) were annotated in an in-house tool conceptually close to the methodology described in [13]. Ten radiologists annotated CT and LDCT images by drawing pericardium contours on axial slices with the help of inter-slice interpolation. At least two readers annotated every study.

We use four datasets to conduct computational experiments; see more details of its usage in Sect. 3.

- *Labeled-LDCT*. 415 annotated LDCT studies. The main training dataset.
- *Labeled-CT*. 76 annotated chest CT studies. An auxiliary dataset to compare pericardium interior segmentation quality for CT and LDCT images.
- *Unlabeled-Paired*. 57 non annotated pairs CT-LDCT; each pair consists of CT study and LDCT study collected from the same subject with no more than 60 days between studies. The primary dataset for experimenting with the second pipeline step - different postprocessing approaches.
- *Labeled-Paired*. 21 annotated pairs CT-LDCT prepared using the same approach as *Unlabeled-Paired*. Hold-out dataset designated exclusively for testing of final models.

Patients cohorts were selected carefully to guarantee zero intersections between datasets and avoid possible data leaks.

3 Experimental Setup

As discussed in Sect. 1, the authors of [2,3] split their method for estimating EAT volume in thoracic CT images into two following consecutive steps.

1. Segmentation of the interior region of the pericardium via CNN.
2. Postprocessing, which includes applying median filter with a 3×3 kernel size to each axial slice of the CT image and calculating the volume of the EAT thresholded as voxels inside pericardium with intensity in range $[l, u] = [-190, -30]$HU. We refer to this postprocessing step as *Median-Thresholding* (l, u).

We aim to adapt and validate this two-step approach in LDCT images. Therefore, we design our experiments as follows.

- First, we train and validate a CNN for PIR segmentation in both low-dose and full-dose CT images. As we show in Sect. 4, this network followed by *Median-Thresholding* $(-190, -30)$ successfully quantifies EAT volume in full-dose CT images. We describe details in Sect. 3.1.
- Then, we use the trained CNN to delineate pericardiums in both low-dose and full-dose CT images from the *Unlabeled-Paired* dataset. For each patient, we quantify EAT inside the predicted pericardium in the full-dose CT image using *Median-Thresholding* $(-190, -30)$. Taking these volumes as ground truth, we calibrate postprocessing step for estimating EAT volumes in the low-dose CT images. See details in Sect. 3.2.
- Finally, we test the CNN followed by the calibrated postprocessing in low-dose CT images from the *Labeled-Paired* dataset. As a ground truth we take EAT volumes calculated in full-dose CT images using manually annotated pericardiums and *Median-Thresholding* $(-190, -30)$.

3.1 Pericardium Interior Region Segmentation

Our network for segmentation of PIR has a 3D U-Net [18] architecture which is a de facto standard for medical image segmentation. We replace plain convolutional layers with residual blocks [6]. In upsampling branch of U-Net, we also replace transposed convolutions with simple trilinear interpolation.

We split all the images from *Labeled-CT* and *Labeled-LDCT* using 5-fold cross-validation in a stratified by dose (low or full) manner. For each split we train a single network on both low-dose and full-dose images. As mentioned in Sect. 2, patients in *Labeled-CT* and *Labeled-LDCT* datasets are unique and do not intersect with each other and with patients from *Unlabeled-Paired* and *Labeled-Paired* datasets. Therefore, training setup excludes overfitting to the validation and test sets.

Before feeding thoracic CT images to the network, we preprocess them in the following steps. First, we crop each axial CT slice to the bounding box of the pixels with intensities greater than -500 HU, which is in fact the body bounding box. Then, we trilinearly interpolate the cropped 3D image, such that resulting image has a $2 \times 2 \times 3$ mm^3 voxel spacing. Finally, we clip intensities to a $[-200, 200]$ HU window and scale them to the $[0, 1]$ range.

We train the network for 15k batches of size 3 using Adam optimizer [10] with default parameters and a learning rate of $3 \cdot 10^{-4}$. As a loss function we use a sum of binary cross entropy and dice loss [14] weighted by 0.1.

To assess the quality of pericardium prediction we calculate the average Dice scores between the network's predictions and the ground truth PIR masks, separately for low-dose and full-dose images, in each validation fold. In Sect. 4.1 we report the mean value and standard deviation of these Dice scores along 5 folds. Also, for each image, we calculate the average Dice score between multiple ground truth masks annotated by different radiologists. In Sect. 4.1 we report the mean values of these inter-rater Dice scores on the *Labeled-CT* and *Labeled-LDCT* datasets as a strong baseline for predictions' Dice scores.

Also, we assess the quality of EAT volume estimation in full-dose CT images using network's pericardium predictions and *Median-Thresholding* $(-190, -30)$. As a ground truth we use EAT volumes calculated using annotated ground truth pericardiums and *Median-Thresholding* $(-190, -30)$. As quality metrics we calculate mean absolute errors, and Pearson's correlation between predicted and ground truth volumes in each validation fold. In Sect. 4.1 we report the mean values and the standard deviations of these metrics along 5 folds. Also, we report the inter-rater mean absolute errors for the ground truth volumes in *Labeled-CT* dataset.

3.2 Postprocessing Calibration for LDCT

A postprocessing step takes a CT image and the PIR mask as inputs and aims to assign 1 to fat voxels inside pericardium, and 0 to other voxels. After that, EAT volume is calculated as a sum of positive voxels' volumes.

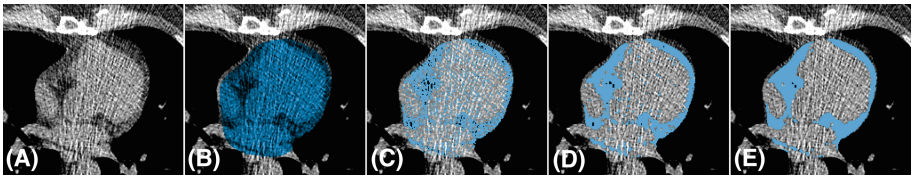

Fig. 1. From left to right: (A) - a patch of an axial low-dose CT slice containing the heart; (B) - the PIR mask predicted via 3D U-Net; (C), (D), and (E) - the fat voxels inside pericardium obtained via *Naïve-Thresholding* $(-190, -30)$, *Median-Thresholding* $(-190, -30)$, and *Gaussian-Thresholding* $(-190, -30, \sigma = 1$ mm), correspondingly.

The most straightforward approach for postprocessing is to exclude voxels with the original CT intensity beyond range $[l, u]$ from the PIR. We refer to this approach as *Naïve-Thresholding* (l, u). However, it results in errors due to noise in CT images, especially low-dose CT images (see Fig. 1(C)). Therefore, in [2,3] authors apply *Median-Thresholding* $(-190, -30)$ as an attempt to eliminate noise effect. We take this approach as a gold standard for full-dose CT images, however, in Sect. 4 we show that it yields poor quality in low-dose CT images. Therefore, we need to adjust the postprocessing step for LDCT. In addition to *Naïve-Thresholding* (l, u) and *Median-Thresholding* (l, u) we also validate the

Gaussian-Thresholding (l, u, σ), which is applying the gaussian filtering with scale σ to the CT image, followed by thresholding voxels inside pericardium to $[l, u]$ range. The simple way to adjust all three aforementioned approaches is to calibrate the parameters (l, u).

To compare different approaches for postprocessing in LDCT, we use the *Unlabeled-Paired* dataset. We predict the PIR masks in both full-dose and low-dose image for each patient using the network described in Sect. 3.1. Then we apply *Median-Thresholding* $(-190, -30)$ to the PIR predictions in full-dose CT images and take the resulting volumes as a ground truth for each patient. After that, we apply *Naïve-Thresholding* (l, u), *Median-Thresholding* (l, u), and *Gaussian-Thresholding* (l, u, σ) for $\sigma \in \{1, 3\}$ mm, for $(l, u) \in \{-300, -290, \ldots, -110, -100\} \times \{-70, -65, \ldots, -15, -10\}$HU to the PIR predictions in LDCT images. For each postprocessing setup we calculate the mean absolute errors between the resulting volumes and the ground truth volumes. Thus, we choose the best setup for postprocessing in LDCT images to fit the ground truth volumes predicted in the corresponding CT images. The results of this calibration are described in Sect. 4.

3.3 EAT Quantification in LDCT

The proposed method for EAT volume estimation in LDCT images consists of PIR segmentation using the network described in Sect. 3.1 and the calibrated postprocessing described in Sect. 3.2.

To finally assess the quality of this method we use the *Labeled-Paired* dataset. For each patient we predict the EAT volume in LDCT image and calculate the ground truth EAT folume in full-dose CT image using the ground truth pericardium annotation and *Median-Thresholding* $(-190, -30)$, following [2,3]. In Sect. 4 we report the mean absolute error and Pearson's correlation between the predicted and ground truth volumes. Also, we report the inter-rater mean absolute errors for the ground truth volumes, as a strong baseline for the quality of EAT volume estimation in the *Labeled-Paired* dataset.

4 Results

4.1 Pericardium Interior Region Segmentation

In Table 1, we report the quality metrics for PIR segmentation in low-dose and full-dose CT images via the network described in Sect. 3.1. As seen, the quality in low-dose CT is as good as quality in full-dose CT. Also we show that the network's error achieves the inter-rater variability.

Also, in the first row of Table 2, we report the quality metrics for the EAT volume estimation in full-dose CT images via the network followed by *Median-Thresholding* $(-190, -30)$. Despite that volume prediction error substantially exceeds the inter-rater volume estimation, we obtained the same mean Pearson's R of 0.97 as authors of [3], and conclude that estimation of EAT volume in full-dose CT images is reliable.

Table 1. Pericardium interior region segmentation Dice scores. We used 5-fold cross-validation for the proposed approach; the numbers are presented as *mean (std)*. Inter-rater variability estimation is based on multiple annotations per image.

Dataset	Proposed	Inter-rater
Labeled-ULDCT	0.95(0.00)	0.95
Labeled-CT	0.95(0.00)	0.96

4.2 Postprocessing Calibration for LDCT

The mean absolute errors between predicted EAT volumes in low-dose and full-dose CT images for the same patients from *Unlabeled-Paired* dataset, for different LDCT-postprocessing setups, are shown in Fig. 2.

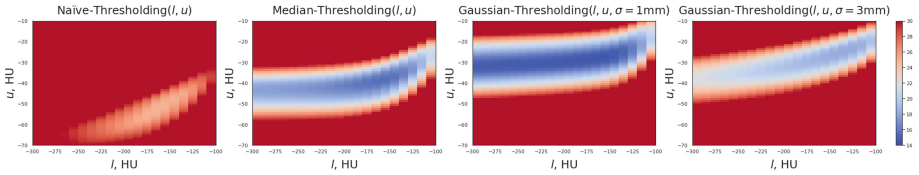

Fig. 2. The mean absolute errors maps on the grid of (l, v) values for the different postprocessing setups. Mean absolute errors are shown by color; colorbar values are given in milliliters.

Gaussian-Thresholding $(l, u, \sigma = 1$ mm) allows to achieve an optimal mean absolute error of 14.54 ml, when setting $(l, u) = (-170, -29)$, while setting the standard fat attenuation range $(l, u) = (-190, -30)$ yields mean absolute error of 14.58 ml. *Median-Thresholding* (l, u) yields the optimal mean absolute error of 15.54 ml, when setting $(l, u) = (-160, -39)$, which significantly differs from the standard range.

Both these optimums are comparable with the error between the unknown true and the predicted, taken as ground truth, EAT volumes in the CT image. Therefore, we cannot conclude that gaussian filtering allows to estimate the EAT volume in LDCT more accurately then median filtering. However, we give preference to the *Gaussian-Thresholding* $(-190, -30, \sigma = 1$ mm) postprocessing, because it achieves the optimal error, while keeping the standard thresholds for the fat voxels.

4.3 EAT Quantification in LDCT

In the second row of the Table 2 we report the quality metrics for the EAT volume estimation via the network, described in Sect. 3.1, followed by *Gaussian-Thresholding* $(-190, -30, \sigma = 1$ mm) postprocessing, chosen as a result of the calibration, described in Sect. 3.2 and Sect. 4.2. As seen, the proposed method achieves the same quality in low-dose CT and full-dose CT images.

Table 2. Epicardial Adipose Tissue quantification metrics. We report Mean Absolute Error (MAE) in milliliters, Pearson's R, and mean Bias between the predicted and the average manually estimated EAT volumes, as well as mean absolute error between multiple manually estimated volumes. The numbers are presented as *mean (std)*. The first row contains the metrics calculated using the 5-fold cross-validation on *Labeled-CT* dataset. The second row compares the network followed by *Gaussian-Thresholding* ($-190, -30, \sigma$ =1 mm) as a model for EAT quantification in LDCTs versus manual estimations in corresponding CTs from the *Labeled-Paired* dataset.

Dataset	EAT volume MAE, ml		Pearson's R	Bias, ml
	Proposed	Inter-rater		
Labeled-CT	14.45(3.14)	9.84	0.97(0.02)	−0.12(6.0)
Labeled-Paired	13.73(0.96)	7.6	0.96(0.01)	2.26(2.46)

5 Discussion

We studied automatic EAT quantification on LDCT images using a large database with more than 500 subjects. Despite poor image quality due to ultra-low dose (less than 1 ms), the proposed combination of classical 3D U-net and postprocessing achieves excellent results. The quality of automatic EAT quantification is almost equal to that for CTs images (Pearson's R 0.96 ± 0.01 and 0.97 ± 0.02 correspondingly). A slightly higher std for CTs can be explained by a much smaller number of full dose studies in the training set (415 vs 76). The obtained scores are aligned with findings in other studeis, e.g. see a large multicenter study [3] where Pearson's R 0.974 was reported.

Another interesting finding shows that a popular postprocessing approach based on the median filter may lead to a systematic shift in HU range of EAT voxels, whereas a Gaussian filter yields better results even within the standard $[-190, -30]$ range. It is important to note that this outcome depends on a particular LDCT protocol and may not be generalized to other protocols (for example, with voltage reduced to 100 kV).

Despite the high quality of the solution, the mean absolute error of our LDCT-based estimation is higher than inter-rater variability on CTs collected from the same subjects (14.45 ± 3.14 and 7.6, correspondingly). Due to several limitations of our study, we can not identify the key contributing factors. Among these limitations, we highlight the interval up to 60 days between the collection of CT and LDCT images for subjects from *Labeled Paired* which could result in systematic differences not related to change in CT dose.

Acknowledgments. This research was supported by the Russian Science Foundation grant 20-71-10134. Computational experiments were powered by Zhores, a super computer at Skolkovo Institute of Science and Technology [20].

References

1. Ambrose, J.A., Singh, M.: Pathophysiology of coronary artery disease leading to acute coronary syndromes. F1000prime reports 7 (2015)
2. Commandeur, F., et al.: Deep learning for quantification of epicardial and thoracic adipose tissue from non-contrast CT. IEEE Trans. Med. Imaging **37**(8), 1835–1846 (2018)
3. Commandeur, F., et al.: Fully automated CT quantification of epicardial adipose tissue by deep learning: a multicenter study. Radiol.: Artif. Intell. **1**(6), e190045 (2019)
4. Ding, J., et al.: The association of pericardial fat with incident coronary heart disease: the multi-ethnic study of atherosclerosis (MESA). Am. J. Clin. Nutr. **90**(3), 499–504 (2009)
5. Flüchter, S., et al.: Volumetric assessment of epicardial adipose tissue with cardiovascular magnetic resonance imaging. Obesity **15**(4), 870–878 (2007)
6. He, K., Zhang, X., Ren, S., Sun, J.: Deep residual learning for image recognition. In: Proceedings of the IEEE Conference on Computer Vision and Pattern Recognition, pp. 770–778 (2016)
7. He, X., et al.: Automatic epicardial fat segmentation in cardiac CT imaging using 3D deep attention U-Net. In: Medical Imaging 2020: Image Processing. vol. 11313, p. 113132D. International Society for Optics and Photonics (2020)
8. Khan, M.A., et al.: Global epidemiology of ischemic heart disease: results from the global burden of disease study. Cureus **12**(7) (2020)
9. Kim, B.J., et al.: Relationship of echocardiographic epicardial fat thickness and epicardial fat volume by computed tomography with coronary artery calcification: data from the Caesar study. Arch. Med. Res. **48**(4), 352–359 (2017)
10. Kingma, D.P., Ba, J.: Adam: a method for stochastic optimization. arXiv preprint arXiv:1412.6980 (2014)
11. Lee, K.C., Yong, H.S., Lee, J., Kang, E.Y., Na, J.O.: Is the epicardial adipose tissue area on non-ECG gated low-dose chest CT useful for predicting coronary atherosclerosis in an asymptomatic population considered for lung cancer screening? Eur. Radiol. **29**(2), 932–940 (2019)
12. Marwan, M., et al.: Quantification of epicardial adipose tissue by cardiac CT: influence of acquisition parameters and contrast enhancement. Eur. J. Radiol. **121**, 108732 (2019)
13. Militello, C., et al.: A semi-automatic approach for epicardial adipose tissue segmentation and quantification on cardiac CT scans. Comput. Biol. Med. **114**, 103424 (2019)
14. Milletari, F., Navab, N., Ahmadi, S.A.: V-net: fully convolutional neural networks for volumetric medical image segmentation. In: 2016 Fourth International Conference on 3D Vision (3DV), pp. 565–571. IEEE (2016)
15. Miyazawa, I., et al.: Change in pericardial fat volume and cardiovascular risk factors in a general population of Japanese men. Circul. J. CJ-18 (2018)
16. Morozov, S., et al.: Moscow screening: lung cancer screening with low-dose computed tomography. Problemy sotsial'noi gigieny, zdravookhraneniia i istorii meditsiny **27**(Special Issue), 630–636 (2019)
17. Nagayama, Y., et al.: Epicardial fat volume measured on nongated chest CT is a predictor of coronary artery disease. Eur. Radiol. **29**(7), 3638–3646 (2019)
18. Ronneberger, O., Fischer, P., Brox, T.: U-net: convolutional networks for biomedical image segmentation. In: International Conference on Medical Image Computing and Computer-Assisted Intervention, pp. 234–241. Springer (2015)

19. Simon-Yarza, I., Viteri-Ramírez, G., Saiz-Mendiguren, R., Slon-Roblero, P.J., Paramo, M., Bastarrika, G.: Feasibility of epicardial adipose tissue quantification in non-ECG-gated low-radiation-dose CT: comparison with prospectively ECG-gated cardiac CT. Acta Radiol. **53**(5), 536–540 (2012)
20. Zacharov, I., et al.: 'Zhores'-petaflops supercomputer for data-driven modeling, machine learning and artificial intelligence installed in Skolkovo institute of science and technology. Open Eng. **9**(1), 512–520 (2019)

Author Queries

Chapter 11

Query Refs.	Details Required	Author's response
AQ1	This is to inform you that corresponding author has been identified as per the information available in the Copyright form.	

MARKED PROOF

Please correct and return this set

Please use the proof correction marks shown below for all alterations and corrections. If you wish to return your proof by fax you should ensure that all amendments are written clearly in dark ink and are made well within the page margins.

Instruction to printer	*Textual mark*	*Marginal mark*
Leave unchanged	··· under matter to remain	New matter followed by
Insert in text the matter indicated in the margin		or (x2)
Delete	through single character, rule or underline or through all characters to be deleted	or (x2)
Substitute character or substitute part of one or more word(s)	through letter or through characters	new character or new characters
Change to italics	under matter to be changed	
Change to capitals	under matter to be changed	
Change to small capitals	under matter to be changed	
Change to bold type	under matter to be changed	
Change to bold italic	under matter to be changed	
Change to lower case	Encircle matter to be changed	
Change italic to upright type	(As above)	
Change bold to non-bold type	(As above)	
Insert 'superior' character	through character or where required	or under character e.g. or
Insert 'inferior' character	(As above)	over character e.g.
Insert full stop	(As above)	
Insert comma	(As above)	
Insert single quotation marks	(As above)	or and/or or
Insert double quotation marks	(As above)	or and/or or
Insert hyphen	(As above)	
Start new paragraph		
No new paragraph		
Transpose		
Close up	linking characters	
Insert or substitute space between characters or words	through character or where required	
Reduce space between characters or words	between characters or words affected	